Preprint
UCRL-JC-134688

OPUS: An Optically Parallel Ultrasound Sensor

J.S. Kallman, A.E. Ashby, D.R. Ciarlo, G.H. Thomas

This article was submitted to
SPIE's International Symposium, Bios 2000, Biomedical Optics, San Jose, CA, January 22-28, 2000

December 13, 1999

OPUS: an optically parallel ultrasound sensor

Jeffrey S. Kallman*, A. Elaine Ashby, Dino R. Ciarlo, Graham H. Thomas

Lawrence Livermore National Laboratory, L-154, Livermore, CA 94550

ABSTRACT

Transmission ultrasound is not in widespread use, partially because of the time and expense of acquiring the data. We are addressing this problem with an optically parallel ultrasound sensor. The core of the sensor is a thin silicon nitride membrane patterned with gold to create "acoustic pixels" over a large area. Each acoustic pixel vibrates at the frequency of the acoustic excitation. The thin membrane, supported by short walls over an optical substrate, with one side immersed in the ultrasound medium and the supported side exposed to air, flexes when an ultrasound pressure wave encounters it. This flexing causes the air gap between the optical substrate and the membrane to change. The change in the air gap modulates the reflection of an optical beam by frustrated total internal reflection. By strobing the optical beam, the deflection of the membrane can be detected and measured at any point through the acoustic period. Acquiring a sequence of images allow us to extract the relative pressure phase and amplitude. Proof of principle experiments have shown that we can build this sensor, and we are currently using a small aperture version to examine simple test objects.

keywords: Optical MEMS, ultrasound, transmission imaging.

1. INTRODUCTION

In 1981 Greenleaf and Bahn[1] published the results of a Mayo Clinic investigation of transmission ultrasonic diagnosis of breast cancer. One of the problems they encountered was the difficulty of obtaining data. Another was the lack of good reconstruction algorithms. There has been significant work done on reconstruction algorithms over the years[2,3], but acquiring the data remains a problem. Our research addresses the acquisition of data for transmission ultrasound imaging. We have invented a sensor which can acquire an entire plane of ultrasound data as a sequence of images. The relevance of this to breast cancer screening is that it can reduce the data acquisition time for transmission ultrasound imaging by three orders of magnitude, compared to mechanical scanning of a point sensor. Arrays of point sensors must be either multiplexed in time (which is slow), or have multiple copies of the necessary electronics to read them (which is expensive). The sensor we are developing addresses these problems. This makes possible a safe (no ionizing radiation), comfortable (no compression), inexpensive (no toxic consumables), and fast screening tool.

Other technologies are currently being developed to optically sense pressure fields over large areas. A dielectric multilayer Fabry-Perot system can be used to modulate the reflection of an optical beam[4]. This sensor works well, but is built to sense pulses with pressures in the megapascal range (multiple atmospheres). A technique based around textured polymer sheets uses frustrated total internal reflection to sense pressure, but it does not have the frequency response necessary to sense ultrasound[5]. Another technique uses the change in refractive index of water with the passage of an ultrasound wave. This technique, however, is sensitive to pulses with peak pressures in the tens to hundreds of megapascals of

*. Correspondence: Email: kallman1@llnl.gov; Telephone: 925 423 2447; Fax: 925 423 3144

pressure (hundreds to thousands of atmospheres)[6]. There is also work being done to sense ultrasound fields in acoustic media by optical tomography[7,8], but these are time consuming.

The basic physical principle we are using to do our ultrasonic sensing is frustrated total internal reflection (FTIR, a consequence of optical refraction)[9]. Refraction occurs when a wave crosses an interface between media in which the speeds of light are different (i.e. of different refractive indices) [Snell's Law]. If light moves from a slow medium to a fast one, there is a critical angle, $\theta_c = \sin^{-1}(n_1/n_2)$ (where n_2 is the index of refraction of the slow medium and n_1 is the index in the fast medium), beyond which the light is totally reflected. This simple picture ignores the evanescent wave, which extends outside the high index medium, falls off exponentially in amplitude to almost zero within one wavelength beyond the interface, and does not propagate. Frustrated total internal reflection occurs when another slow medium intercepts the evanescent wave. Some light tunnels through the gap and propagates into that medium. The amount of light that tunnels is related to the materials involved, the polarization, and the gap width.

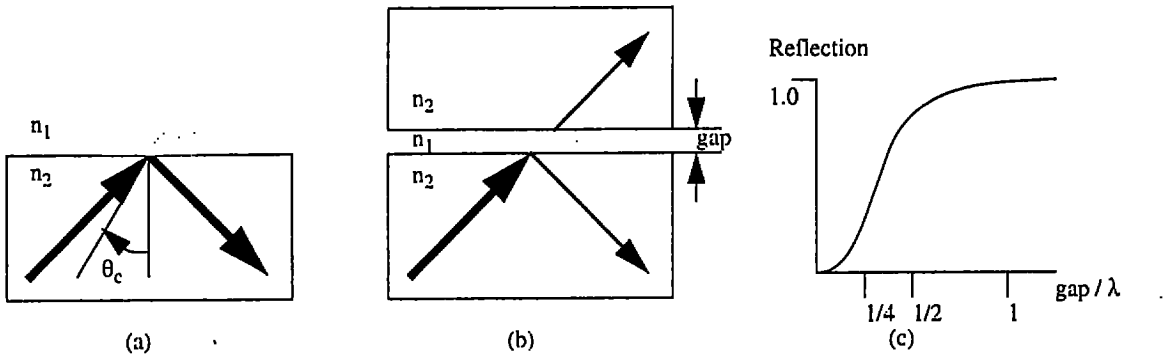

Figure 1. (a) Total internal reflection (TIR) occurring at the interface between an optically slow medium (n2) and a fast medium (n1). The evanescent wave extends into the fast medium. (b) Frustrated total internal reflection occurs when another slow medium intercepts the evanescent wave. (c) Reflection vs. gap size.

Our new sensor uses FTIR to make an incident ultrasonic wave modulate a pulsed beam of light, which is then acquired by a camera and computer. A sequence of images, each taken with the optical pulse at a different source acoustic phase, enables us to reconstruct the ultrasonic phase and amplitude over an entire 2-D surface.

In this paper we detail the development and design of our optically parallel ultrasound sensor (OPUS).

2. OPTICS

We can exploit FTIR by building an array of acoustic pixels. Each acoustic pixel is composed of a thin (0.1 micron) silicon nitride membrane suspended on short (0.2 micron) gold walls over an optical substrate. The gap between the membrane and the optical substrate is filled with air (figure 2). The membrane is exposed to the ultrasonic couplant. When an ultrasonic pressure wave travels through the couplant and impinges on the acoustic pixel, the membrane deflects, causing a change in the amount of light reflected from the total internal reflection surface of the acoustic pixel. An array of acoustic pixels can be used to modulate a beam of light.

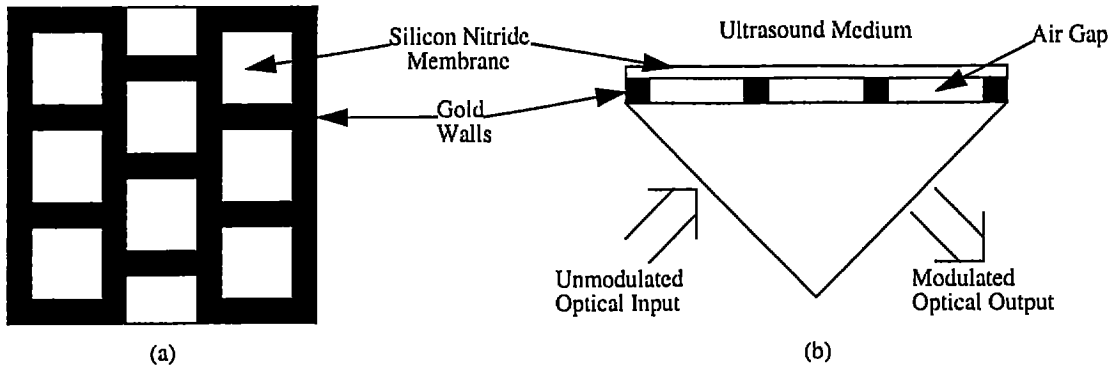

Figure 2. (a) Top view of an array of acoustic pixels. (b) Side view showing acoustic pixels mounted on optical substrate

Given a continuous light source we could use a photodiode to monitor the modulation of the reflected beam, but we would need a photodiode per acoustic pixel and multiplexed electronics to use this technique. An alternative is to use a strobed light source and a digital camera to take a sequence of images that allow us to extract the phase and amplitude of the vibration of the entire set of acoustic pixels. Just as a strobe light can be used to watch the vibration of a drumhead, we are using a strobed source to watch the relative phases and amplitudes of tens of thousands of tiny drumheads, all at once. Given a sequence of images and calibration data, we can extract the relative phase and amplitude of the vibration, and thus extract the relative pressure phase and amplitude at each acoustic pixel. To obtain this information we illuminate the sensor with ten sequences of optical pulses, each sequence timed to act as a strobe light at a specific acoustic phase (figure 3).

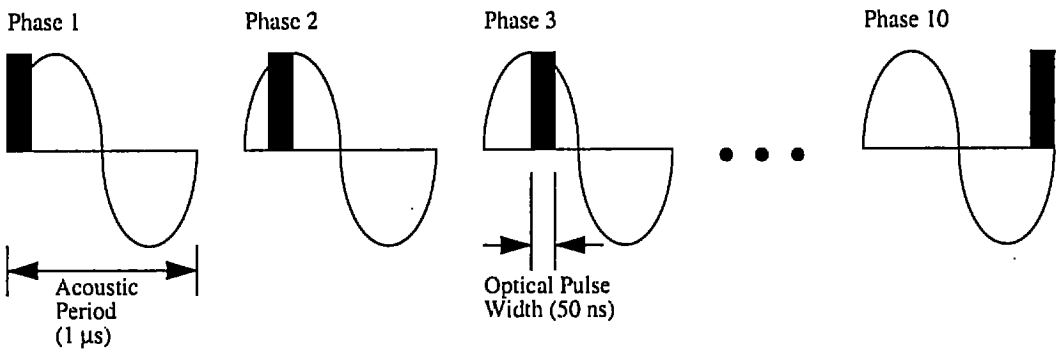

Figure 3. Ten images are taken, each with the optical pulse at a different position in the acoustic period. At an acoustic frequency of 1 MHz, a 1 second camera exposure will collect 1 million pulses.

We extract the phase and amplitude at each pixel by fitting the intensity at that pixel through the sequence to the form $I = B + A \sin(2 \pi i / 10 + C)$ where I is the intensity, B is the background, A is the amplitude of the sinusoidal variation, i is the index of the image in the sequence, and C is the phase of the variation.

The optical train of this device is as follows: we illuminate the sensor using an LED, the light from which is homogenized, polarized, and collimated. We acquire the reflection using a CCD still camera.

3. ACOUSTICS

The imaging technique we are interested in is transmission ultrasound. In this modality, an acoustic source sends out a pressure wave through a couplant, such as water, oil, or medical ultrasound gel, to the

object of interest. The pressure waves are transmitted through the object, being modified in amplitude and phase along the way. The pressure wave emerges from the object of interest and travels, via the couplant, to our acoustic sensor.

Our sensor works because the pressure wave flexes a membrane, causing it to vibrate with a phase and amplitude that are functions of that wave. In designing our sensor, we needed to have a membrane with a frequency response high enough to vibrate at the frequencies of interest to us (approximately 1 MHz).

4. DESIGN PARAMETERS

There are many material and operational parameters that must be chosen correctly in order to make a working OPUS. Among these are the membrane and wall materials, membrane thickness, wall height, acoustic pixel size, ultrasound operating frequency, optical source characteristics, optical pulse characteristics, and camera characteristics.

Some of these parameters were simple to choose, such as the material for the membrane. The fabrication processes available to us restricted our choice of membrane materials to silicon and silicon nitride. As we wanted to do this work with visible light, we chose to use a silicon nitride membrane

Other parameters were more difficult to choose, as there was significant interaction between them. For instance, the membrane thickness and the acoustic pixel size interact with each other to effect the sensitivity and frequency response of the sensor. Thus, we relied on modeling to narrow the ranges of these parameters.

5. MODELING

We began our work on this project by modeling as many of the systems and processes as possible. We used an in-house reduced-dimension finite-difference time-domain Maxwell's solver (TSARLITE)[10] to model the optical aspects of the sensor (FTIR), a 3-D mechanical dynamics code (DYNA3D)[11] to model the acoustic responses of the membranes and their supports, and a reduced-dimension Beam Propagation Method code (BEEMER)[10] to model the imaging system as a whole.

Using TSARLITE we were able to determine the ranges where we could expect FTIR to be useful, and bounded the permissible thickness of the membrane and the heights of the supports it would stand upon. This aspect of the modeling was performed to ensure that we would be able to engineer to the physical phenomenon we were utilizing.

BEEMER was used to examine the issues that arise when the sensor is used for diffraction tomographic imaging. It was used to model the tomographic data acquisition process, as well as a number of reconstruction algorithms.

The simulation program used most heavily was DYNA3D. We used this program to model our initial sensor design, a membrane suspended on an array of posts. DYNA3D showed that this design had neither the sensitivity nor the frequency response necessary to allow us to acquire the data we required. Guided by our simulations, we developed a more responsive design, a set of resonant membranes suspended on walls. Simulation showed this design was responsive and sensitive, but had problems with cross-talk and drift of the resonant frequency as a function of hydrostatic pressure (see Figure 4). Further simulation allowed us to modify the design by offsetting the cells and varying their size so as to greatly reduce cross-talk (see Figure 5).

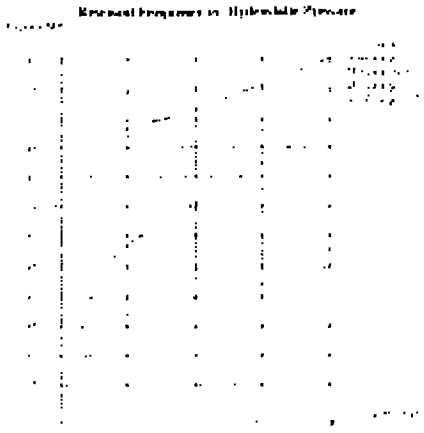

Figure 4. DYNA3D simulation led to these curves of expected resonant frequency with respect to hydrostatic pressure.

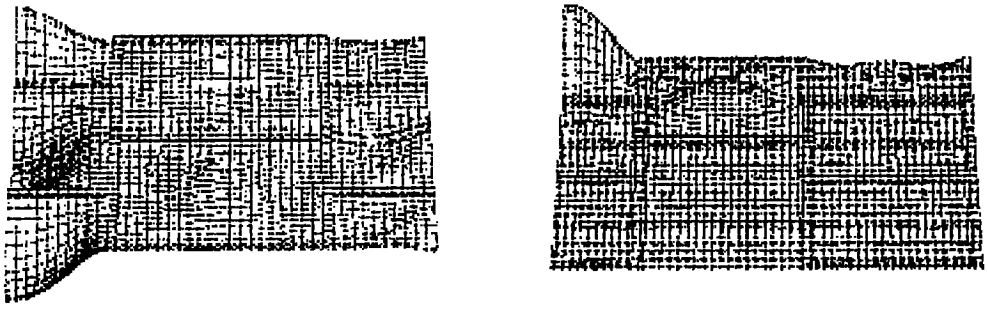

Figure 5. Simulation showed crosstalk between acoustic pixels to be a problem. Staggering the acoustic pixels as in (a) reduces the crosstalk, but additionally staggering the resonant frequencies of the acoustic pixels as in (b) reduces the crosstalk significantly.

Simulation led us to a reasonable first design, but we still needed to do experiments to verify the simulations, and get proof of principle results. To do these experiments we built a test system.

6. FABRICATION

The membrane and its supports are fabricated as depicted in Figure 6:

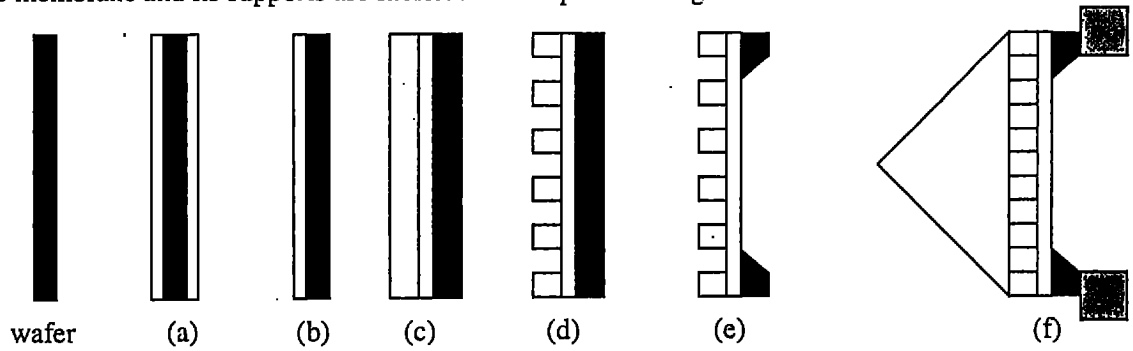

Figure 6. (a) The silicon wafer has nitride deposited on both sides. (b) The nitride is etched away on one side. (c) A layer of gold is deposited on the nitride. (d) The gold is etched except where it will be support walls. (e) The silicon is etched from the back, except for a frame that supports the whole system. (f) The membrane and walls are mated to the optical substrate , and then mounted to the support plate.

7. PROOF OF PRINCIPLE

The test system consisted of a test membrane, a tank with an acoustic source, and the optics. The test membrane was designed to allow us to examine the responses of a wide range of membrane resonator sizes to variations in hydrostatic pressure. The rest of the system was designed to make all of the parameters of interest easily available for manipulation.

The test membrane consists of a 1 cm square membrane of silicon nitride, supported by gold walls, held in a silicon frame. The gold walls were patterned as shown in figure 7. On the left hand side of the test membrane are alternating rows of 60 acoustic pixels ranging in size from 0.02 mm to 0.08 mm on a side. On the right hand side of the test membrane only half of the rows are populated with acoustic pixels. The reason for the wide range in size is evident from the simulation results in figure 4.

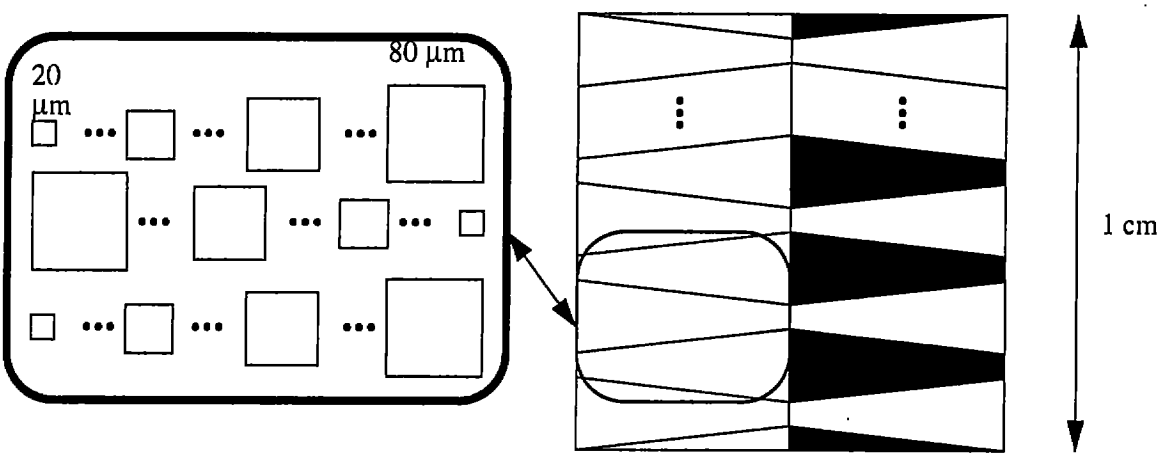

Figure 7. The layout of the acoustic pixels in the proof of principle test membrane.

We suspected that only acoustic pixels that were at the exact resonant frequency would be sensitive enough to modulate the optical input, and so we attempted to include all pertinent sizes. In addition to the wide range in resonator sizes available, we had membrane fabrication parameters available for modification as well (membrane thickness and gold wall height).

The remainder of the system is illustrated in schematic form in figure 8. The oscillator provides a 1 MHz CW signal, which is amplified and fed through the power meter to the acoustic source in the water tank. The same signal goes to the pulse generator, which in turn excites the optical source as a strobe light. The pulse generator output and the oscillator output are both fed to an oscilloscope to allow the user to place the optical pulse at any point in the acoustic phase. The optical pulses are homogenized, polarized, collimated, and fed through the prism to the sensing surface, and the reflected light is captured by the camera and saved in the computer. The user has control over the oscillator frequency, the amplifier gain, the camera exposure time, the optical pulse width, amplitude, and placement in the acoustic phase, as well as the depth of the water in the tank.

During a typical experimental run with this proof of principle system the water tank was filled to the desired depth, and the acoustic power level, camera exposure time, optical pulse width, and optical pulse amplitude are set. Sequences of ten images are acquired, each with the optical pulse occurring at a different acoustic phase.

We learned a great deal using the test system, most importantly that: 1) we can engineer to the sizes and tolerances necessary to use the physical phenomenon; 2) we can extract phase and amplitude data at each acoustic pixel from sequences of images; 3) the resonances are broad enough that acoustic pixel size is non-critical; and 4) hydrostatic pressure causes little change in membrane response.

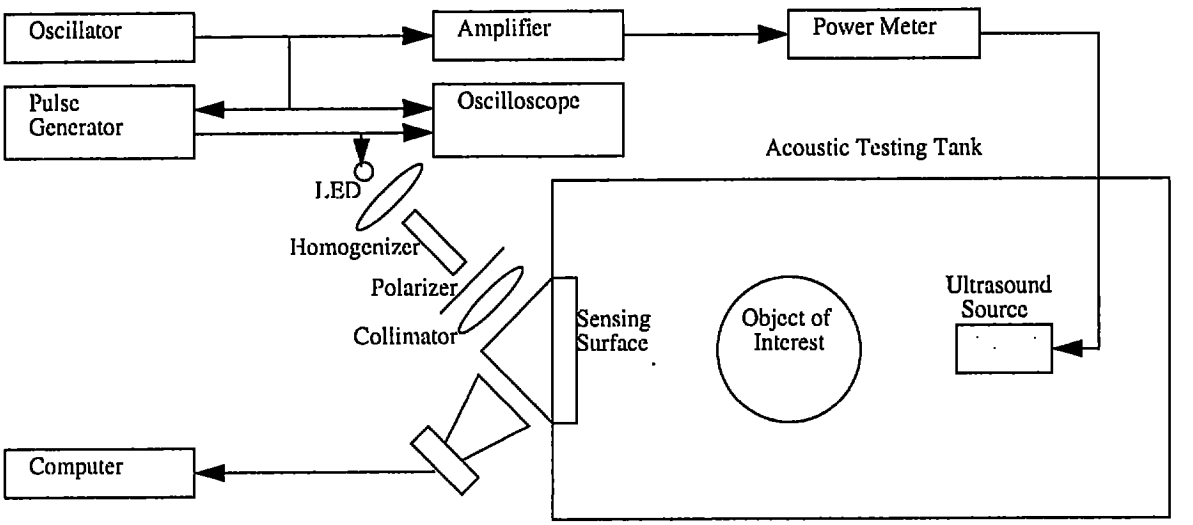

Figure 8. Schematic view of the data acquisition system. The oscillator output is sent to the amplifier (to provide the acoustic signal to the transducer) and the pulse generator (to provide the optical signal). The optical pulse is homogenized, polarized, collimated and sent to the sensing surface. Upon reflection it is acquired by the computer controlled camera. The object of interest is optional. In the test system (where we were interested in membrane responses) there was no object of interest.

After performing numerous experimental runs we were able to arrive at a set of design parameters for an actual sensor.

8. SENSOR PARAMETERS

As a result of the proof-of-principle experiments, we had the information necessary for the design and fabrication of the first generation sensor. The cell size is 70 microns square, with a 0.1 micron thick membrane, mounted on walls 0.2 microns high. The active aperture is 7 mm square. The sensor is being operated at a frequency of 1MHz, at an acoustic power of 0.02 Watts/cm^2.

9. SENSOR NOISE CHARACTERISTICS

The CCD camera we are using is an Apogee Instruments AP1. The images it provides are 760 x 510 pixels, each of which is 16 bits deep. We expose the CCD for one second (one million pulses). We are using a HP 214B pulse generator to send 50 nanosecond 5 volt pulses to a red LED.

To determine the purely optical noise characteristics of our data, we collected a set of 40 images with no acoustic excitation. The noise is approximately Gaussian with standard deviations extending from 24 to 60 counts. In taking data, with the acoustic and optical parameters as above, we collect 36 sequences of images and average, reducing the noise by a factor of 6. The expected sinusoidal variation in our data had amplitudes ranging from 30 to 100 counts.

10 . DATA

For data collection we used the same tank and optics as for the proof of principle experiments. Because data acquisition is not yet fully automated, and to make the best use of data storage capacity, we collected 36 sequences of 10 images, with no target (calibration), a 1mm radius garnet bead, and a 1.5mm radius coral bead.

10.1 Data acquisition

Each series of images was acquired as follows: the optical pulse (50ns) was placed at the beginning of the acoustic period and an image was acquired. For the next image, the optical pulse was moved forward 100ns. This was repeated until the entire acoustic period was uniformly sampled (10 images).

10.2 Data reduction

The 36 images at each phase (for the calibration and for both targets) were averaged together pixel by pixel, yielding 3 averaged sequences of 10 images. For every pixel in each sequence, the intensity was fit to a sinusoid with phase plus a background. Since the illumination over the optical field was not uniform (intentionally, to minimize costs), the sinusoidal amplitude was normalized by the background intensity. For every pixel in each of the three sequences we recorded the amplitude ratio and the phase. To extract relative pressure amplitude, we normalize the image of the target ratios by the image of the calibration ratios, on a pixel by pixel basis. This yielded two images of relative pressure amplitude. By subtracting the calibration phase from the target phases, we obtained two images of relative phase. See Figures 9 and 10.

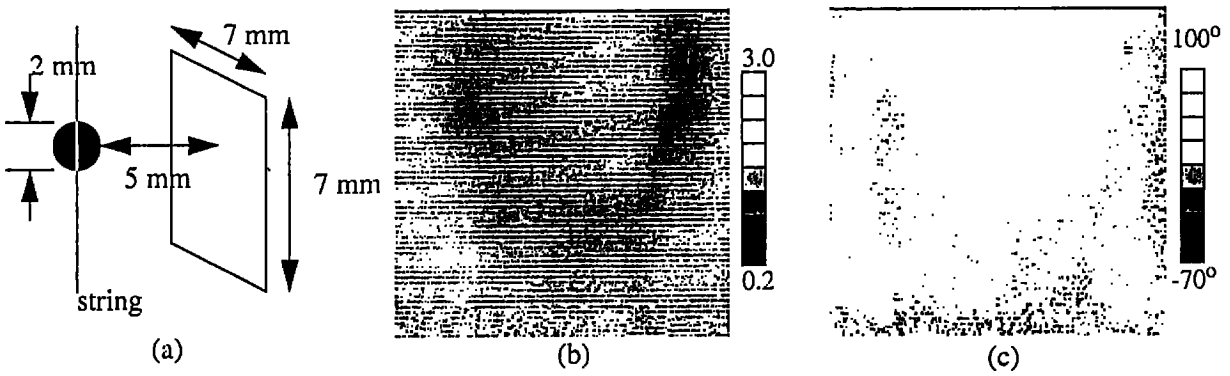

Figure 9. Relative pressure amplitude and phase with garnet bead as target. (a) experimental setup, (b) relative amplitude image, (c) relative phase image.

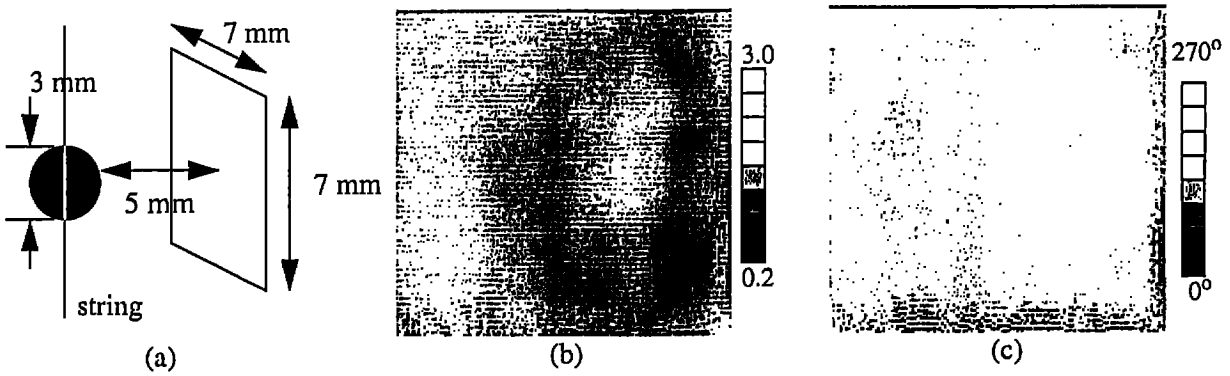

Figure 10. Relative pressure amplitude and phase with coral bead as target. (a) experimental setup, (b) relative amplitude image, (c) relative phase image.

Note that these are raw data, not reconstructions of the spheres. To fully reconstruct these phantoms would require more data, and much more processing. It is, however, evident from these data that the targets are visible to the 1.4mm wavelength ultrasound and that the sensor can see the effects that these targets have on the acoustic field.

11. SUMMARY

We have developed a new type of ultrasound sensor that makes it possible to sense the pressure field over a plane. The sensor uses the phenomenon of frustrated total internal reflection to modulate the reflection of an optical beam depending on the deflection of a 0.1 micron thick silicon nitride membrane that covers an acoustic pixel. Our acoustic pixels are defined by gold walls 0.2 microns tall and enclosing a square air space approximately 70 microns on a side. We have successfully used a 0.7 cm square array of approximately 10,000 acoustic pixels to acquire relative pressure amplitude and phase images of garnet and coral beads.

12. FUTURE WORK

12.1. Automation

We are in the process of making data acquisition completely automatic. This entails the computer control of the pulse positioning in the acoustic period. When finished, this automation will enable more rapid (and less human effort intensive) data acquisition.

12.2. Scaling challenges

In order to make this sensor useful for industrial and medical applications, we are scaling up the sensing aperture for the OPUS. There are two challenges that arise in this work. The first is the difficulty of building large free standing membranes. We are circumventing that difficulty by building mosaics of 0.7 cm windows. Another challenge is the large depth of focus necessary to collect data over the entire sensor surface. Currently, we are working with a small enough sensing surface that the entire surface can be kept in focus all at once. As we scale up the sensor it will be necessary to change the mounting of the lens to our camera (so as to tilt the back of the camera and keep the focused image on the camera's ccd).

ACKNOWLEDGEMENTS

This work was performed under the auspices of the U.S. Department of Energy by Lawrence Livermore National Laboratory under contract W-7405-Eng-48.

REFERENCES

1. J. F. Greenleaf and R. C. Bahn, "Clinical Imaging with Transmissive Ultrasonic Computerized Tomography," *IEEE Trans. on Biomedical Engineering*, **BME-28**, pp. 177-185, 1981.
2. A. J. Devaney, "A filtered backpropagation algorithm for diffraction tomography," *Ultrasonic Imaging*, **4**, pp. 336-350, 1982.
3. K. T. Ladas and A. J. Devaney, "Generalized ART algorithm for diffraction tomography," *Inverse Problems*, **7**, pp. 109-125, 1991.
4. V. Wilkens and Ch. Koch, "Optical multilayer ditection array for fast ultrasonic field mapping," *Optics Letters*, **24**, pp. 1026-1028, 1999.

5. M. Mitchell, M. Howarth, C. R. Gentle, "Production and evaluation of textured polymer sheets as optical pressure-sensing interfaces," *J. Materials Processing Technology*, **77**, pp. 129-133, 1998.
6. G. Paltauf, H Schmidt-Kloiber, K. P. Kostli, M. Frenz, "Optical method for two-dimensional ultrasonic detection," *Appl. Phys. Lett.*, **75**, 1048-1050, 1999.
7. G. Yao and L. V. Wang, "Full-field mapping of ultrasonic field by light-source-synchronized projection," *J Acoust. Soc. Am.*, **106**, pp. L36-L40, 1999.
8. M. Almqvist, A. Holm, T. Jansson, H. W. Persson, K. Lindstrom, "High resolution light diffraction tomography: nearfield measurements of 10 MHz continuous wave ultrasound," *Ultrasonics*, **37**, pp. 343-353, 1999.
9. P. Yeh, *Optical Waves in Layered Media*, John Wiley and Sons, New York, 1988.
10. R. J. Hawkins, J. S. Kallman, R. W. Ziolkowski, "Computational Integrated Photonics," *Engineering Research Development and Technology*, R. T. Langland, C. Minichino, UCRL 53868-92, pp 1.7-1.11, Lawrence Livermore National Laboratory, LIvermore, 1993.
11. R. G. Whirley, B. E. Engelmann, *A Nonlinear, Explicit, Three-Dimensional Finite Element Code For Solid and Structural Mechanics - User Manual*, Lawrence Livermore National Laboratory, Livermore, 1993.